Journal of Molecular Graphics and Modelling 34 (2012) 38–45

Contents lists available at SciVerse ScienceDirect

Journal of Molecular Graphics and Modelling

journal homepage: www.elsevier.com/locate/JMGM

Energies and physicochemical properties of cation–π interactions in biological structures

Qi-Shi Du[a,b,c,*], Jian-Zong Meng[b], Si-Ming Liao[a,b], Ri-Bo Huang[a,b]

[a] State Key Laboratory of Non-food Biomass Energy and Enzyme Technology, National Engineering Research Center for Non-food Biorefinery, Guangxi Academy of Sciences, 98 Daling Road, Nanning, Guangxi 530007, China
[b] State Key Laboratory for Conservation and Utilization of Subtropical Agro-bioresources, Life Science and Biotechnology College, Guangxi University, Nanning, Guangxi 530004, China
[c] Gordon Life Science Institute, San Diego, CA 92130, USA

ARTICLE INFO

Article history:
Received 13 August 2011
Received in revised form
14 December 2011
Accepted 15 December 2011
Available online 29 December 2011

Keywords:
Cation–π interaction
Quantum chemistry
Molecular modeling
Protein structures
Structural biology

ABSTRACT

The cation–π interactions occur frequently within or between proteins due to six (Phe, Tyr, Trp, Arg, Lys, and His) of the twenty natural amino acids potentially interacting with metallic cations via these interactions. In this study, quantum chemical calculations and molecular orbital (MO) theory are used to study the energies and properties of cation–π interactions in biological structures. The cation–π interactions of H^+ and Li^+ are similar to hydrogen bonds and lithium bonds, respectively, in which the small, naked cations H^+ and Li^+ are buried deep within the π-electron density of aromatic molecules, forming stable cation–π bonds that are much stronger than the cation–π interactions of other alkali metal cations. The cation–π interactions of metallic cations with atomic masses greater than that of Li^+ arise mainly from the coordinate bond comprising empty valence atomic orbitals (AOs) of metallic cations and π-MOs of aromatic molecules, though electrostatic interactions may also contribute to the cation–π interaction. The binding strength of cation–π interactions is determined by the charge and types of AOs in the metallic cations. Cation–π interaction energies are distance- and orientation-dependent; energies decrease with the distance (r) and the orientation angle (θ). In solution, the cation–π energies decrease with the increase of the dielectric constant (ε) of the solvent; however, solvation has less influence on the H^+–π and H_3O^+–π interactions than on interactions with other cations. The conclusions from this study provide useful theoretical insights into the nature of cation–π interactions and may contribute to the development of better force field parameters for describing the molecular dynamics of cation–π interactions within and between proteins.

1. Introduction

The cation–π interaction is increasingly recognized as an important noncovalent molecular interaction relevant to the fields of chemistry and biology [1–6]. Numerous studies have reported cation–π interactions occurring frequently within protein structures [7–10], in protein–ligand interactions [11–15], and in protein–protein and protein–DNA complexes [16–18]. In many cases, the cation–π interaction is the dominant factor in the process of host-ligand recognition within biological structures [7,11,18–20].

Of the twenty natural amino acids, these six have the potential to be involved in cation–π interactions: tryptophan (Trp), tyrosine (Tyr), phenylalanine (Phe), histidine (His), arginine (Arg), and lysine (Lys). Four of these (Phe, Tyr, Trp, and His) possess aromatic motifs in their side chains, and three of the six (Arg, Lys, and His) are often protonated and exist as 'organic cations' in proteins. Histidine can participate in cation–π interactions as either a cation or as a π-motif, depending on its protonation state. A protein database search showed that the cation–π interaction can occur every 77 amino acid residues of proteins [2,10]. Approximately half of the protein complexes and one-third of the homodimers analyzed were found to contain at least one intermolecular cation–π pair [7]. Considering that metallic cations such as Na^+, K^+, Ca^{2+}, Mg^{2+}, Fe^{2+}, and Cu^{2+} are present in many enzymes, the frequency of cation–π interactions in proteins is probably even high [3,19].

Cation–π interactions are unique biomolecular binding forces that occur between electron-rich aromatic rings and organic or inorganic (metallic) cations. This type of noncovalent interaction can be very strong, as has been confirmed by solid-state studies of small-molecule crystal structures [21,22] and by theoretical and experimental analyses in gas phase and in aqueous media [11,21]. The strength of cation–π interactions ranges

* Corresponding author at: State Key Laboratory of Non-food Biomass Energy and Enzyme Technology, National Engineering Research Center for Non-food Biorefinery, Guangxi Academy of Sciences, 98 Daling Road, Nanning, Guangxi 530007, China. Tel.: +86 771 250 3931; fax: +86 771 250 3908.
E-mail address: qishi_du@yahoo.com.cn (Q.-S. Du).

1093-3263/$ – see front matter © 2011 Elsevier Inc. All rights reserved.
doi:10.1016/j.jmgm.2011.12.002

between 10 and 150 kcal/mol [2], which is comparable to the three other major types of molecular interactions: hydrogen bonds, van der Waals interactions, and electrostatic interactions (or salt bridges). Cation–π interactions are therefore considered to be an essential force in generating tertiary and quaternary protein structures induced by oligomerization and protein folding [23].

The cation–π interaction was first reported in the 1940s, and to date, numerous publications have been written on the topic [8,10,11,21,24–30], though some aspects of the cation–π interaction remain unclear. Initially, the cation–π interaction was thought to be a special type of hydrogen bond known as an 'aromatic hydrogen bond' [20,26,31]. This designation, however, does not satisfactorily describe the metallic cation–π interaction. Common hydrogen bonds are point-to-point interactions between hydrogen bond donors and hydrogen bond acceptors, whereas cation–π interactions are point-to-group interactions, in which the cation interacts with an aromatic motif comprising several atoms. Some authors later suggested that the cation–π interaction is primarily an electrostatic interaction [11–16,31–34] between the cation and the π-electron density of the aromatic motif. In the aromatic molecules the π-electron density is a conjugated system, which cannot be described as the electrostatic interactions among negative and positive charges (atoms). Therefore the cation–π interaction energy cannot be evaluated using the Coulomb equation. The cation–π interaction was then described as a polarization interaction, in which a dipole moment is induced from the π-electron density of the aromatic motif by the cation [17]. Typically, polarization is merely a correction to the electrostatic interaction and only has a minor contribution to bond strength; however, the cation–π interactions have the same strength as hydrogen bonds and salt bridges.

To better evaluate cation–π interactions using molecular dynamics (MD) and protein modeling approaches, specially designed force field parameters for the cation–π interactions are required [34]. In this study, we describe a theoretical evaluation of cation–π interactions using quantum chemical calculations and molecular orbital (MO) theory. Our results provide a more detailed description of the properties of cation–π interactions and a greater theoretical insight into the chemical nature of these interactions than has been previously developed.

2. Theory and methods

All calculations are performed on a Sugon-5000 computer using the Gaussian 09 software package [35]. All molecular geometries are optimized using two methods: HF/6-311+G(d,p) and B3LYP/6-31+G(d,p). The former is used for MO analysis and the latter for cation–π interaction energies. The cation–π energies are adjusted at key points using the higher-level method CCSD/TZVP [36–39]. To observe the detailed interactions between different cations and aromatic motifs in organic molecules, the potential surfaces of cation–π interactions are scanned in molecular spaces at 0.05 Å steps using the B3LYP/6-31+G(d,p) method. In this study, the cations analyzed include H^+, H_3O^+, Li^+, Na^+, K^+, Mg^{2+}, Ca^{2+}, and the organic cation $CH_3NH_3^+$. The aromatic molecules, chosen for having different electron-withdrawing groups, electron-inductive groups, and sizes of conjunctive π-motifs, include C_6H_6, $C_6H_5NO_2$, C_6H_5Cl, $C_6H_5CH_3$, C_6H_5OH, $C_6H_5C_6H_5$, and $C_{10}H_{10}$. The distance dependence and orientation dependence of the cation–π interactions are calculated at several directions, and the physical and chemical nature of cation–π bonds is studied using MO theory. The cation–π interactions in different solvation environments are studied using the polarizable continuum model (PCM) [40–43].

3. Results and discussion

All calculation results are reported and summarized in this section using tables and figures. Brief illustrations and comparisons are provided following the calculation results.

3.1. Potential energy surfaces between cations and benzene

Cation–π interactions may occur on the π-plane of aromatic molecules and not at a particular atom. Potential energy surface scanning is a powerful tool for evaluating detailed information in the molecular interaction system. The cation–π interaction potential surfaces of H^+–benzene, Li^+–benzene, Na^+–benzene, and Ca^{2+}–benzene are scanned on an 8 Å × 8 Å plane, which is parallel to the π-plane of aromatic molecules at the optimized distances. The scanning step is 0.05 Å with 25,921 total potential points in each scanning surface. At each potential point, the geometry of benzene and the (*X*, *Z*) coordinates of the cation are fixed, leaving the *Y* coordinate (the distance between cation and π-plane) of the cation to be optimized. The B3LYP/6-31+G(d,p) method is used for potential surface scanning because it is an otherwise time-consuming and computation-intensive process. The cation–π interaction potential surfaces of H^+–benzene and Li^+–benzene are shown in Fig. 1.

As shown in Fig. 1(A), the cation–π interaction of the H^+–benzene system in the gaseous phase is extremely strong. An interesting observation is that there is a peak (−116 kcal/mol) at the center of the concave potential surface, and surrounding the peak is a deep circular groove. The potential groove overlaps the π-electron density of the benzene ring, and six deep potential wells (−168 kcal/mol) are located in the circular groove above the nuclei of the carbon atoms.

Potential surface scanning for the Li^+–benzene interaction system also produces interesting results, as shown in Fig. 1(B). In the concave potential surface, the strongest interaction (−41 kcal/mol) is at the center of the benzene ring 1.94 Å above the π-plane. Surrounding the central potential are six potential peaks, resembling a volcano. Outside of this 'volcano-like' ring, there are six minor potential wells (−28 kcal/mol) that overlap the π-electron density-rich regions of benzene.

The potential surfaces of the Na^+–benzene and Ca^{2+}–benzene interaction systems are shown in Fig. 2. Both potential surfaces of Na^+–benzene and Ca^{2+}–benzene are smooth and concave. The only potential well (minimum) is at the center of the benzene ring. The cation–π interaction energy of Ca^{2+}–benzene (−69 kcal/mol) is much larger than that of Na^+–benzene (−27 kcal/mol).

A comparison between Fig. 1 and Fig. 2 reveals that the cation–π interactions of H^+ and Li^+ are clearly different from the cation–π interactions of other metallic cations (Na^+ and Ca^{2+}), suggesting that the physicochemical nature and interaction behavior of H^+ and Li^+ also differs from other metallic cations.

3.2. Orientation dependence and distance dependence of cation–π interactions

Cation–π interactions do not necessarily occur perpendicular to the aromatic π-plane; they could occur in any direction. To study the orientation dependence and distance dependence of cation–π interactions, we calculate the interaction potential curves as a function of distance (r) and orientation angle (θ). The results of these calculations are shown in Fig. 3. The 'zeta' (θ) is the angle between the direction of the cation–π interaction and the perpendicular from the plane of the benzene ring, while the distance (r) is measured from the position of the cation to the center of the benzene ring. For both Li^+–benzene and Na^+–benzene, the most favorable direction for cation–π interactions is perpendicular to the center of

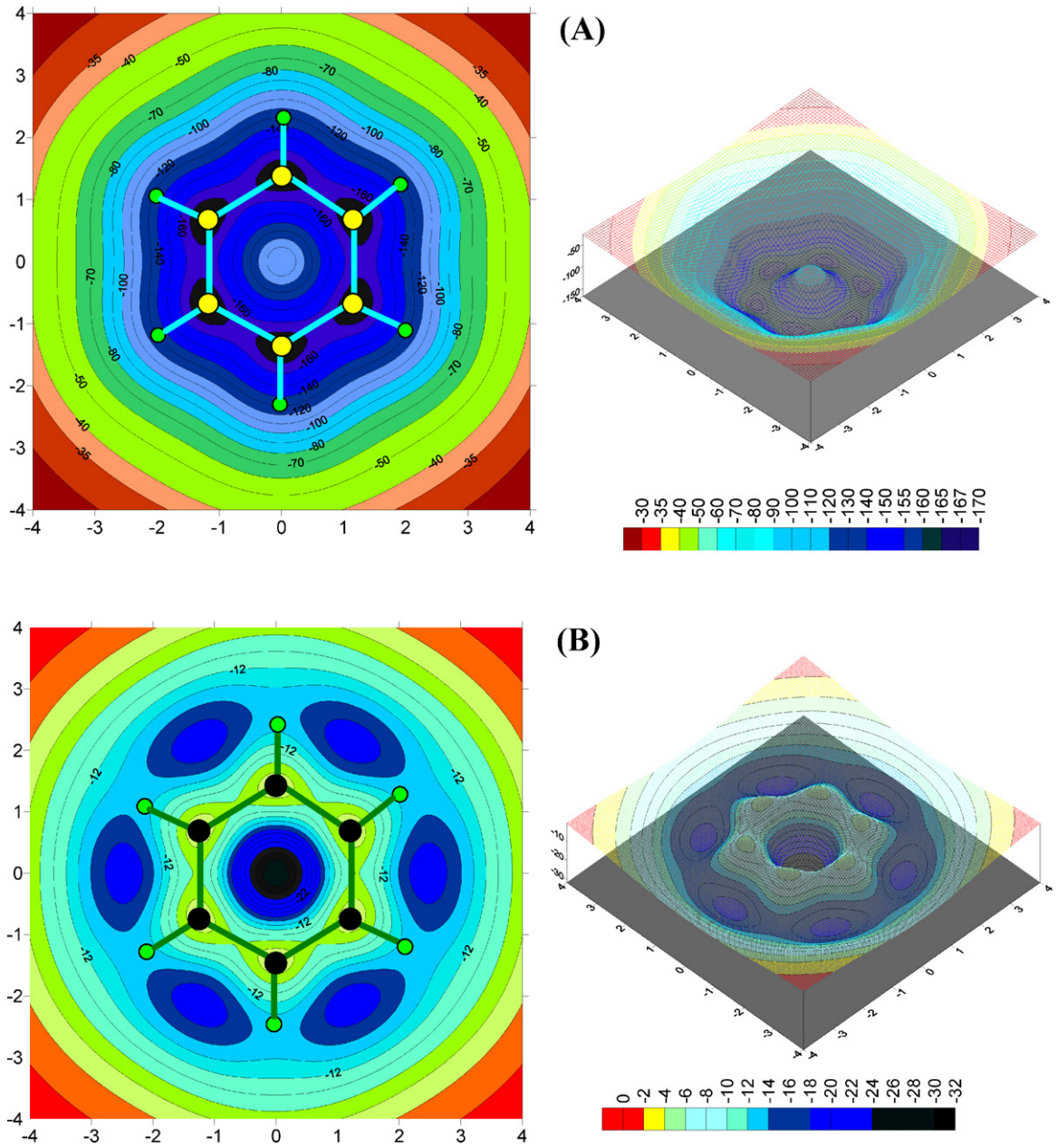

Fig. 1. Potential surfaces of cation–π interactions. (A) Cation–π interaction of H^+–benzene. In the center of the concave potential surface, there is a peak (−116 kcal/mol). Surrounding the peak is a deep, circular potential groove that overlaps the π-electron density of the benzene ring and six deep potential wells (−168 kcal/mol) located in the circular groove above the carbon nuclei. (B) Cation–π interaction of Li^+–benzene. For Li^+–benzene, the strongest interaction is in the center (−41 kcal/mol) of the benzene ring; however, there are six minor potential wells (−28 kcal/mol) at the π-electron density.

the benzene ring ($\theta = 0^\circ$). However, for the H^+–benzene interaction, the most favorable direction is between $\theta = 40^\circ$ and $\theta = 50^\circ$.

3.3. Molecular orbitals of cation–π interactions

The nature of the chemical bond of cation–π interactions can be revealed by quantum chemical calculations based on MO theory. Fig. 4 shows the highest occupied molecular orbital (HOMO) of H^+–benzene, Li^+–benzene, Na^+–benzene, and Ca^{2+}–benzene interaction systems.

As shown in Fig. 4(A), the naked proton (H^+) is deeply buried in the π-electron density of benzene. This positioning is analogous to the hydrogen bond, in which the naked proton is buried in the electron density of an electronegative element (e.g., oxygen and nitrogen). Fig. 4(B) shows that the cation Li^+ is also trapped in the π-electron density of benzene. Thus, the Li^+–π interaction is similar to the 'lithium bond' [44,45], in which the cation Li^+ is trapped in the electron density of an electronegative element. Lithium, as a congener of hydrogen, participates in similar interactions to form the lithium bond, as hydrogen does to form the hydrogen bond [44,45], though lithium bond energy is usually weaker than the hydrogen bond. The proton H^+ is a small, naked nucleus with no inner electrons, allowing it to be deeply buried in the π-electron density of benzene ($r = 0.973$ Å), yielding a very strong cation–π interaction. The bond length of Li^+–benzene (1.940 Å), however, is much longer than that of H^+–benzene because of the repulsive interaction between 1s electrons of Li^+ and the π-electrons of aromatic molecules.

An interesting result, shown in Fig. 4(C) and (D), is that new MOs are formed between Na^+ and benzene and between Ca^{2+}

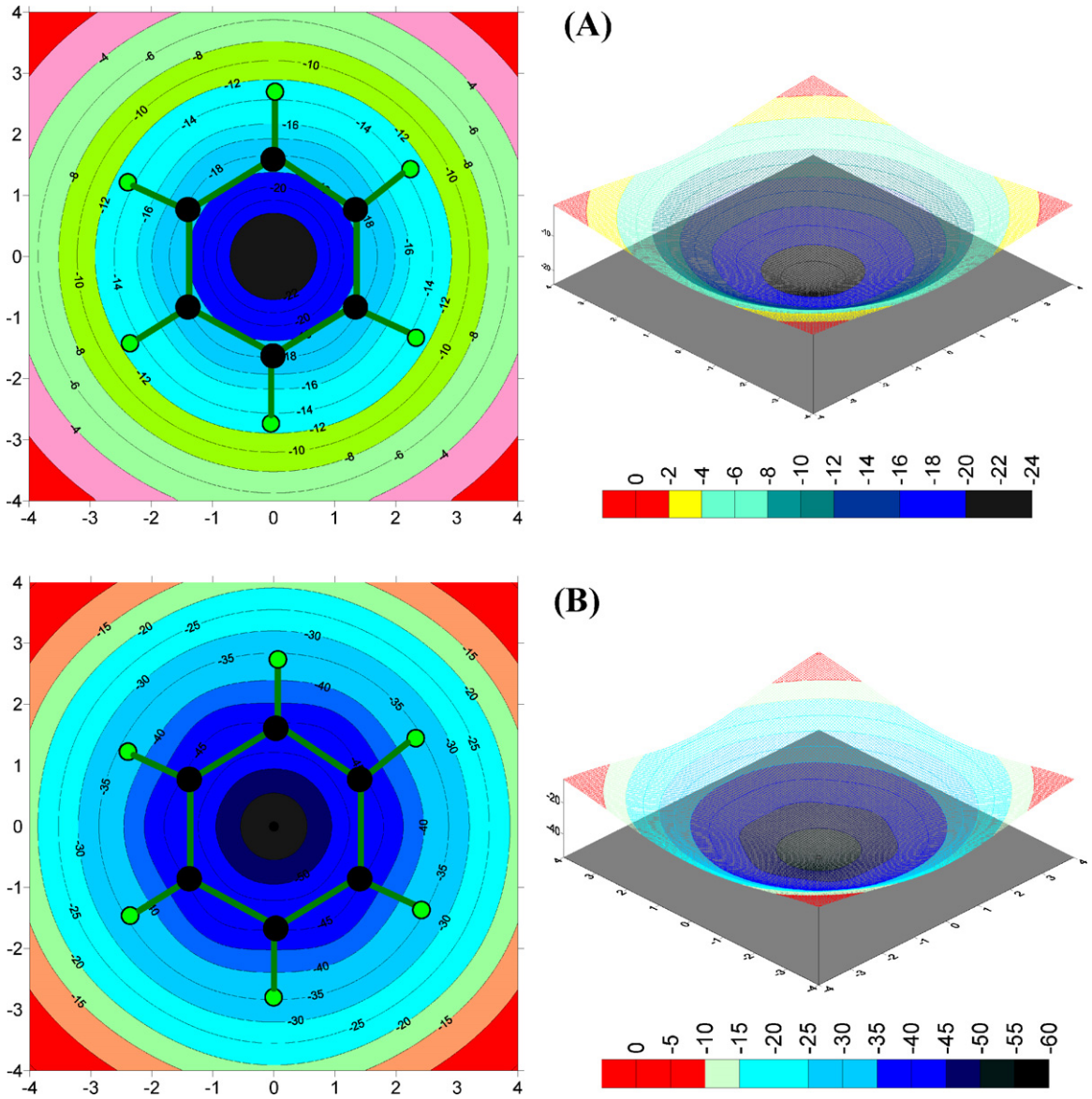

Fig. 2. Potential surfaces of cation–π interactions. (A) Cation–π interaction of Na^+–benzene. The potential surface of Na^+–benzene is perfectly smooth and concave. The only potential well (−27 kcal/mol) is in the center of the benzene ring. (B) Cation–π interaction of Ca^{2+}–benzene. Like Na^+–benzene, the potential surface of Ca^{2+}–benzene is a smooth concave, and the potential well is in the center. However, the cation–π interaction energy (−69 kcal/mol) of Ca^{2+}–benzene is much larger than that of Na^+–benzene.

and benzene. In the Na^+–benzene system, the new MO is composed of a 2p AO of Na^+ and a π–MO of benzene, while in the Ca^{2+}–benzene system, the new MO is formed by a 3d AO of Ca^{2+} and a π–MO of benzene. Because the 3d AOs of Ca^{2+} form bonding MOs more favorably with benzene than do the 2p AOs of Na^+, the cation–π interaction energy of Ca^{2+}–benzene (−69 kcal/mol) is much stronger than that of Na^+–benzene (−27 kcal/mol). Fig. 4(E) and (F) shows the interaction between the organic cation $CH_3NH_3^+$ and benzene. The three polar hydrogen atoms are perpendicular to the π-plane and point to the center of the benzene ring. Unlike the free proton, the polar hydrogen atoms in $CH_3NH_3^+$ are kept at a distance (3.140 Å) from the π-plane due to the repulsive interaction between the π-electron density and the electron density of other atoms in the organic cations.

3.4. Cation–π interaction energies

The cation–π interaction energies and bond lengths between specific cations and aromatic molecules are summarized in Table 1. The cation–π interactions of free protons (H^+) and hydrated protons (H_3O^+) differ both in interaction energy and in bond length. The former interactions only occur in the gaseous phase, while the latter occur in aqueous solution. Based on calculation results presented in Table 1, the electron-inductive groups (—CH_3 and —OH) have only a small influence on the cation–π interaction energy. However, the influence of electron-withdrawing groups (—NO_2 and —Cl) is much larger than that of the electron-inductive groups. In particular, the —NO_2 group reduces the cation–π interaction energy by 1/2–2/3 of the original value. One possible explanation for this reduction is that the atomic group —NO_2 joins the conjunctive π-system and withdraws considerable π-electron density from the benzene ring. If the substituents extend the conjunctive π-system, from C_6H_6 to $C_6H_5C_6H_5$, the interaction energy of Na^+ is 23.35% higher. However, the cation–π interaction energies of most cations have no remarkable increase. The interaction energy of H_3O^+ even decreases with the increase of π-systems.

There exists some controversy in the literature about the effect of solvent on cation–π interaction energies [8,10,12]. In Table 2, the

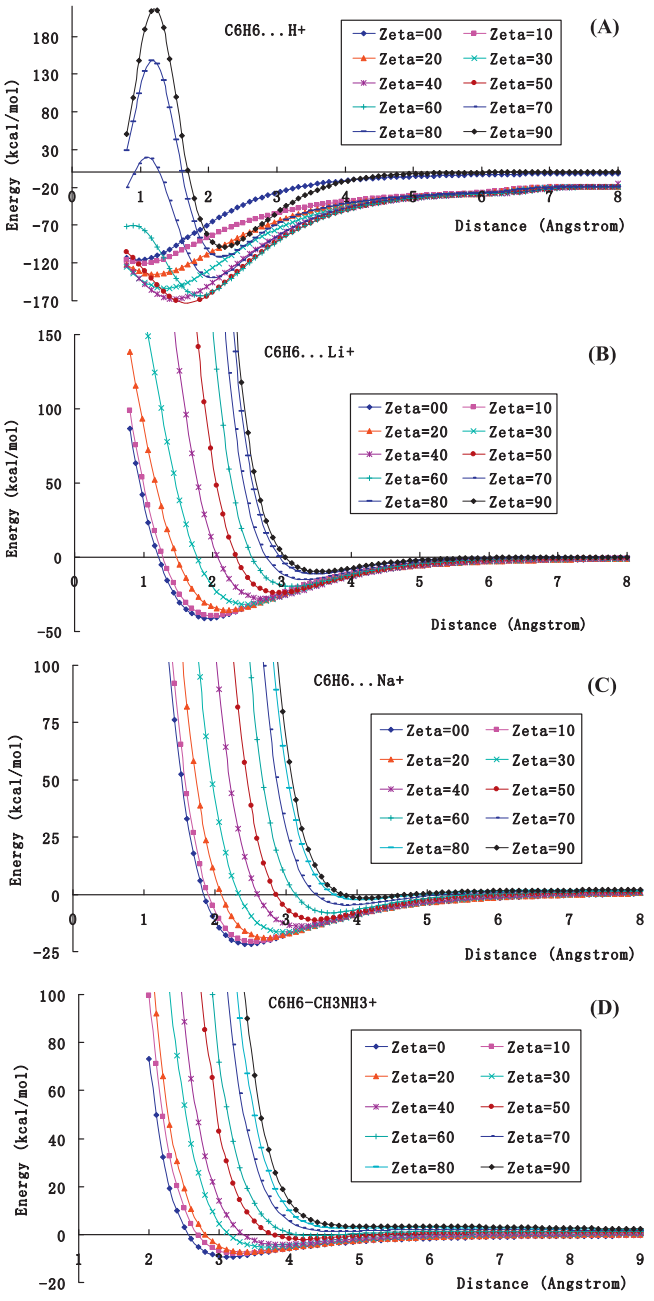

Fig. 3. The orientation dependence and distance dependence of cation–π interactions. Zeta (θ) is the angle between the interaction direction and the perpendicular from the center of benzene ring. (A) Cation–π interaction between H^+ and benzene. (B) Cation–π interaction between Li^+ and benzene. (C) Cation–π interaction between Na^+ and benzene. (D) Cation–π interaction between $CH_3NH_3^+$ and benzene.

cation–π interaction energies, which are calculated using the PCM method [40–43], between benzene and cations in three different solvents are listed. In polar solvents, such as water (ε = 78.39) and acetonitrile (ε = 35.9), the cation–π interaction energies of metallic cations decrease sharply. In aqueous solutions, the cation–π interaction energies of Li^+, Na^+, and Ca^{2+} are reduced by merely −1.0 to −2.0 kcal/mol. However, the solvent effect on free protons (H^+) and hydrated protons (H_3O^+) is much smaller than the effect on other cations (e.g., Li^+, Na^+, and Ca^{2+}). Table 2 shows that the interaction energy of H_3O^+–benzene in aqueous solution is −16.12 kcal/mol, which is much higher than the typical hydrogen bond energy of water molecules (−4 to −6 kcal/mol). This solvent effect is similar to what is seen in the hydrogen bond, highlighting the chemical similarities of the cation–π interaction of protons and the hydrogen bond.

Table 1
Cation–π interaction energies between cations and aromatic molecules.

Vacuum	H^+		H_3O^+		Li^+	
ε = 1.0	Energy[a]	Length[b]	Energy	Length	Energy	Length
C_6H_6	−116.08[c]	0.973	−22.54	3.024	−41.02	1.940
$C_6H_5CH_3$	−120.80	0.973	−18.91	3.001	−39.29	1.922
C_6H_5OH	−120.00	0.991	−17.00	2.969	−39.95	1.948
$C_6H_5NO_2$	−94.10	0.992	−6.508	3.169	−15.21	2.021
C_6H_5Cl	−110.62	0.982	−13.42	3.011	−33.66	1.971
$C_6H_5C_6H_5$	−128.73	1.150	−19.12	2.945	−43.80	1.923
$C_{10}H_{10}$	−126.56	1.146	−19.40	2.951	−42.36	1.927

Vacuum	Na^+		K^+		Mg^{2+}	
ε = 1.0	Energy[a]	Length[b]	Energy	Length	Energy	Length
C_6H_6	−27.06	2.448	−17.14	2.978	−118.69	1.987
$C_6H_5CH_3$	−24.91	2.450	−18.04	2.960	−121.78	2.002
C_6H_5OH	−26.29	2.454	−16.85	3.053	−119.86	1.986
$C_6H_5NO_2$	−8.96	2.560	−6.226	3.141	−83.81	2.026
C_6H_5Cl	−21.36	2.487	−12.81	3.032	−108.15	1.995
$C_6H_5C_6H_5$	−33.38	2.431	−18.35	2.954	−133.00	1.958
$C_{10}H_{10}$	−28.51	2.428	−18.62	2.954	−131.28	1.944

Vacuum	Ca^{2+}		$CH_3NH_3^+$	
ε = 1.0	Energy[a]	Length[b]	Energy	Length
C_6H_6	−68.78	2.151	−12.15	3.140
$C_6H_5CH_3$	−69.30	2.511	−12.93	3.130
C_6H_5OH	−66.29	2.512	−14.04	3.250
$C_6H_5NO_2$	−34.70	2.577	−11.26	3.460
C_6H_5Cl	−59.42	2.529	−8.758	3.210
$C_6H_5C_6H_5$	−78.95	2.475	−13.16	3.120
$C_{10}H_{10}$	−77.69	2.460	−13.53	3.130

[a] kcal/mol.
[b] From cation to the center of benzene ring, in Angstrom (Å).

4. Discussion

Cation–π interactions are a unique type of molecular interaction that cannot be classified into other categories, such as electrostatic or polarization interactions. However, cation–π interactions may contain contributions from other types of molecular interactions. The physical and chemical nature of cation–π interactions for different cations cannot be explained using only one theory. The cation–π interactions of H^+ and Li^+ are similar to the hydrogen bond and lithium bond, respectively [44,45]. The small, naked H^+ and Li^+ cations are buried in the π-electron density, forming a stable cation–π bond. Because H^+ is a small and purely naked nucleus, containing no inner electron, the H^+–π interaction is much stronger than the Li^+–π interaction. The cation Li^+ bears inner 1s electrons,

Table 2
Cation–π interaction energies between cations and benzene in solutions.

C_6H_6 + cation	Water (ε = 78.39)		Acetonitrile (ε = 35.9)		Cyclohexane (ε = 2.0)	
	Energy[a]	Length[b]	Energy[a]	Length[b]	Energy[a]	Length[b]
H^+	−65.70	0.977	−66.55	0.977	−92.12	0.972
H_3O^+	−16.12	3.227	−5.72	3.223	−8.62	3.038
Li^+	−1.70	3.217	−1.70	3.156	−14.30	2.068
Na^+	−1.51	3.453	−1.58	3.436	−10.69	2.585
K^+	−1.72	3.303	−1.84	3.286	−7.764	3.140
Mg^{2+}	+6.26	2.666	+5.61	2.653	−44.11	2.095
Ca^{2+}	−1.07	3.744	−4.60	4.112	−19.86	2.701
$CH_3NH_3^+$	−0.851	3.425	−0.939	3.410	−5.454	3.235

[a] kcal/mol.
[b] From cation to the center of benzene ring, in Angstrom (Å).

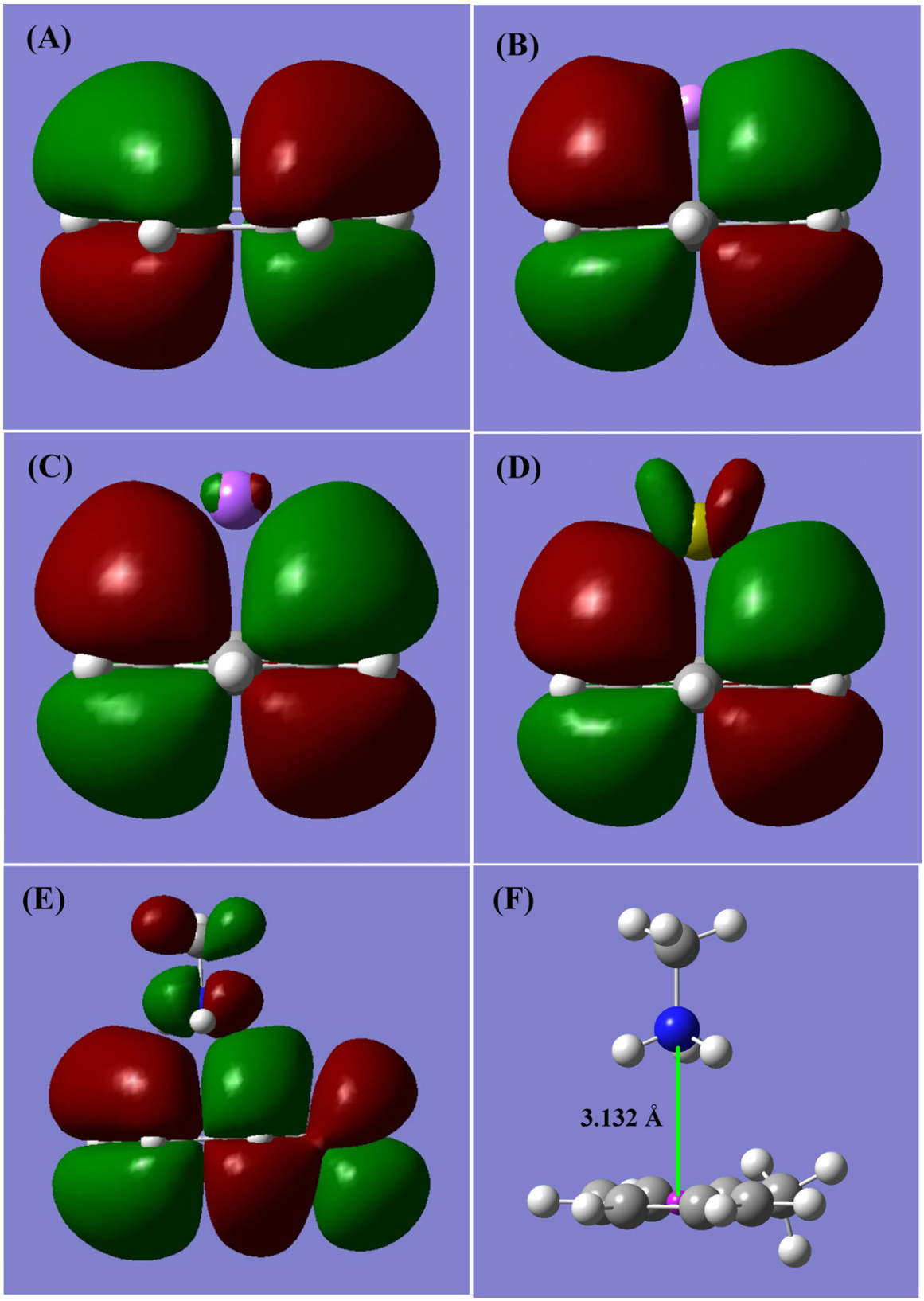

Fig. 4. The highest occupied molecular orbitals (HOMO) of cation–π interaction systems. (A) HOMO of H^+–benzene. The naked proton (H^+) is deeply buried in the π-electron density of benzene, yielding a high interaction energy (−116.08 kcal/mol, r = 0.973 Å). (B) HOMO of Li^+–benzene. Like the proton (H^+), the small cation Li^+ is trapped in the π-electron density of benzene. (C) HOMO of Na^+–benzene. A new MO is formed between the Na^+ cation and benzene. (D) HOMO of Ca^{2+}–benzene. A new MO is also formed between Ca^{2+} and benzene. Because the 3d AOs of Ca^{2+} are more favorable for coordinate MO formation with the π–MO of benzene than the 2p AOs of Na^+, the cation–π interaction energy of Ca^{2+}–benzene (−69 kcal/mol) is much stronger than that of Na^+–benzene (−24 kcal/mol). (E) HOMO of $CH_3NH_3^+$–$C_6H_5CH_3$. (F) Optimized geometry of the $CH_3NH_3^+$–$C_6H_5CH_3$ interaction system. In the organic cation $CH_3NH_3^+$, the proton H^+ is attached (or fixed) in the atomic group. The organic cation is kept at a distance (3.132 Å) from the π-electron density because of the repulsive force from the electron density of the other atoms. The cation–π interaction energy of $CH_3NH_3^+$–$C_6H_5CH_3$ is −12.93 kcal/mol, which is much smaller than that of the free proton H^+.

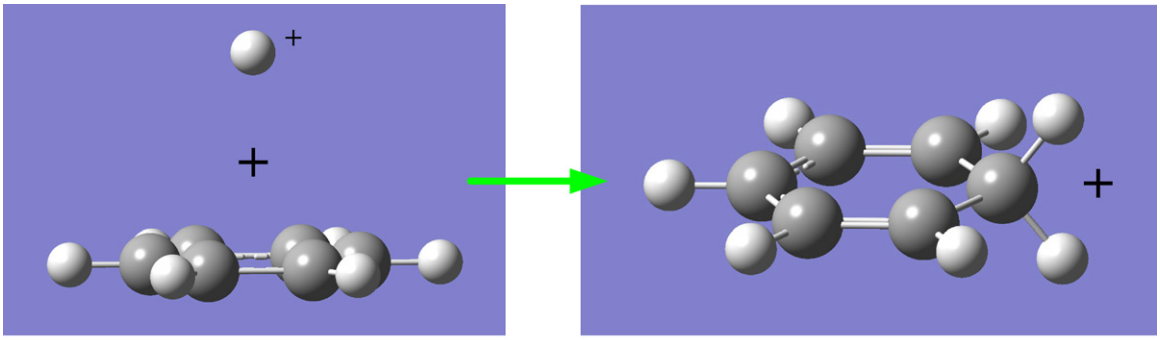

Scheme 1. Geometry optimization of the H^+–benzene system results in a chemical reaction. The final product is protonated benzene ($C_6H_7^+$), and the reaction heat in the gaseous phase is −198.13 kcal/mol.

which may cause a repulsive interaction with the π-electron density of the aromatic motif.

As shown in Fig. 1(A), the strongest H^+–π interaction (−168 kcal/mol) is not located in the center of the benzene ring, but in the six potential wells at the π-electron-rich zone above the carbon nuclei in the benzene ring. The strong H^+–π interaction energy far exceeds the range of common molecular interaction energies. In fact, a full geometry optimization of the H^+–benzene system results in a chemical reaction in which the final product is protonated benzene ($C_6H_7^+$), with a heat of reaction of −198.13 kcal/mol in the gaseous phase, as shown in Scheme 1.

The H^+–π interaction energy of free protons is as high as −116.08 kcal/mol, above the center of benzene ring. In proteins, the behavior of protonated amino acids (His, Arg, and Lys) differs from that of free protons and cannot produce so high an interaction energy. In protonated amino acids, the proton is attached to an atomic group and cannot reach the aromatic motif as closely as a free proton (0.973 Å) because of the repulsive force between the π-electron density and the electron density from other atoms in the amino acid. Conversely, the interaction energy (−16.12 kcal/mol) and bond length (3.227 Å) of H_3O^+–benzene, as shown in Table 2, may represent the actual cation–π interaction of hydrated protons (H_3O^+) in solution.

The cation–π interactions of other metallic cations (with greater atomic mass than Li^+) result primarily from the formation of new MOs, as shown in Fig. 3 (C) and (D), implying that coordinate bonds are formed. The strength of cation–π bonds depends on the charge and the atomic valence orbital type of the metallic cation. However, the cation–π interaction energies may contain contributions from electrostatic interactions and polarization interactions. The interaction energy of Mg^{2+} provides a good evidence that electrostatic interactions contribute to cation–π interactions. The larger cation–π energy of Mg^{2+}–C_6H_6 (−118.69 kcal/mol) than that of Na^+–C_6H_6 (−27.06 kcal/mol) can be explained by the higher charge of Mg^{2+} than the charge of Na^+. The higher cation–π energy of Mg^{2+} than the energy of Ca^{2+} (−68.78 kcal/mol) cannot be explained by the bonding ability of 2d AO and 3d AO, may be explained by the higher ionic potential of Mg^{2+}. Clearly, unknown factors affecting cation–π interactions remain to be studied.

In solution, the cation–π interactions of all cations other than H^+ and H_3O^+ decrease sharply with the increase of the solvent dielectric constant. However, the solvent effect on the proton H^+ and H_3O^+ is smaller. In the complex structure of proteins in aqueous solution, hydrophilic residues are located at the surface and are exposed to solvent, while hydrophobic residues are hidden inside the hydrophobic core of the protein. In the hydrophobic cavity, the dielectric constant is much smaller than in the bulk of aqueous solution; therefore, the cation–π interaction likely still occurs in proteins.

5. Conclusion

Based on the calculation results presented in this study, some useful conclusions can be drawn. (1) Cation–π interaction energies are in the range of 10–150 kcal/mol, which is comparable to hydrogen bonds and salt bridges. (2) The cation–π interactions of H^+ and Li^+ have different physical and chemical properties than cation–π interactions with other metallic cations. The small, naked cations H^+ and Li^+ are buried deeply in the π-electron density, forming special cation–π bonds. (3) In the cation–π interactions of metallic cations with greater atomic mass than Li^+, new MOs are formed between the valence AOs of metallic cations and MOs of π-conjugated systems. The strength of cation–π interactions is determined by the charge and valence AO type of the metallic cation. (4) Cation–π interactions are distance- and orientation-dependent and are point-to-group interactions. The most favorable interaction direction is perpendicular to the conjugated π-plane. For H^+, however, the most favorable interaction direction is between $\theta = 40^\circ$ and $\theta = 50^\circ$ to the π-plane. (5) Cation–π interactions are subject to the solvent effect, which decreases with the increase of the solvent dielectric constant. However, solvent has less effect on the cation–π interactions of H^+ and H_3O^+ than on interactions with other cations.

The interaction properties and the energies of cation–π interactions, revealed in this study, enrich our understanding of the physicochemical nature of cation–π interactions. The conclusions drawn from this study provide useful theoretical insights into the nature of cation–π interactions and may help to develop better force field parameters for describing the molecular dynamics of cation–π interactions within and between proteins.

Acknowledgements

This work is financially supported by the National Science Foundation of China (NSFC) under the project 30970562 and 31160032, and by the Guangxi Natural Science Foundation under the project 2010GXNSFD013030.

Appendix A. Supplementary data

Supplementary data associated with this article can be found, in the online version, at doi:10.1016/j.jmgm.2011.12.002.

References

[1] S.A. Pless, K.S. Millen, A.P. Hanek, J.W. Lynch, H.A. Lester, S.C.R. Lummis, D.A. Dougherty, A cation–π interaction in the binding site of the glycine receptor is mediated by a phenylalanine residue, J. Neurosci. 28 (2008) 10937–10942.

[2] U.D. Priyakumar, M. Punnagai, G.P. Krishna Mohan, G.N. Sastry, A computational study of cation–π interactions in polycyclic systems: exploring the dependence on the curvature and electronic factors, Tetrahedron 60 (2004) 3037–3043.

[3] A.S. Reddy, G.N. Sastry, Cation, [M = H^+, Li^+ Na^+, K^+, Ca^{2+}, Mg^{2+}, NH^{4+}, and NMe^{4+}] interactions with the aromatic motifs of naturally occurring amino acids: a theoretical study, J. Phys. Chem. A 109 (2005) 8893–8903.

[4] D.A. Dougherty, Cation–π interactions involving aromatic amino acids, J. Nutr. 137 (2007) 1504S–1508S.

[5] B.L. Schottel, H.T. Chifotides, K.R. Dunbar, Anion–π interactions, Chem. Soc. Rev. 37 (2008) 68–83.

[6] S.K. Burley, G.A. Petsko, Amino–aromatic interactions in proteins, FEBS Lett. 203 (1986) 139–143.

[7] P.B. Crowley, A. Golovin, Cation–π interactions in protein–protein interfaces, Proteins 59 (2005) 231–239.

[8] J.C. Ma, D.A. Dougherty, The cation–π interaction, Chem. Rev. 97 (1997) 1303–1324.

[9] N.S. Scrutton, A.R.C. Raine, Cation–π bonding and amino–aromatic interactions in the biomolecular recognition of substituted ammonium ligands, Biochem. J. 319 (1996) 1–8.

[10] J.P. Gallivan, D.A. Dougherty, Cation–π interactions in structural biology, Proc. Natl. Acad. Sci. U.S.A. 96 (1999) 9459–9464.

[11] E.A. Meyer, R.K. Castellano, F. Diederich, Interactions with aromatic rings in chemical and biological recognition, Angew Chem. Int. Ed. 42 (2003) 1210–1250.

[12] C. Biot, E. Buisine, M. Rooman, Free-energy calculations of protein–ligand cation–π and amino–pi interactions: from vacuum to protein-like environments, J. Am. Chem. Soc. 125 (2003) 13988–13994.

[13] D.A. Dougherty, Cation–π interactions in chemistry and biology: a new view of benzene, Phe, Tyr, and Trp, Science 271 (1996) 163–168.

[14] M.M. Flocco, S.L. Mowbray, Planar stacking interactions of arginine and aromatic side chains in proteins, J. Mol. Biol. 235 (1994) 709–717.

[15] T.M. Fong, M.A. Cascieri, H. Yu, A. Bansal, C. Swain, C.D. Strader, Amino–aromatic interaction between histidine 197 of the neurokinin-1 receptor and CP 96345, Nature 362 (1993) 350–353.

[16] R. Wintjens, J. Lievin, M. Rooman, E. Buisine, Contribution of cation–π interactions to the stability of protein–DNA complexes, J. Mol. Biol. 302 (2000) 395–410.

[17] M. Rooman, J. Lievin, E. Buisine, R. Wintjens, Cation–π/H-bond stair motifs at protein–DNA interfaces, J. Mol. Biol. 319 (2002) 67–76.

[18] J.S. Lamoureux, J.T. Maynes, J.N.M. Glover, Recognition of 5-YpG-3_sequences by coupled stacking/hydrogen bonding interactions with amino acid residues, J. Mol. Biol. 335 (2004) 399–408.

[19] C. Janiak, A critical account on π–π stacking in metal complexes with aromatic nitrogen-containing ligands, J. Chem. Soc. Dalton Trans. (2000) 3885–3896.

[20] C.A. Hunter, K.R. Lawson, J. Perkins, C.J. Urch, Aromatic interactions, J. Chem. Soc. Perkin Trans. 2 (2001) 651–669.

[21] D. Zhu, B.E. Herbert, M.A. Schlautman, E.R. Carraway, Characterization of cation–π interactions in aqueous solution using deuterium nuclear magnetic resonance spectroscopy, J. Environ. Qual. 33 (2004) 276–284.

[22] R.A. Kumpf, D.A. Dougherty, A mechanism for ion selectivity in potassium channels: computational studies of cation–π interactions, Science 261 (1993) 1708–1710.

[23] L. Brocchieri, S. Karlin, Geometry of interplanar residue contacts in protein structures, Proc. Natl. Acad. Sci. U.S.A. 91 (1994) 9297–9301.

[24] D.A. Dougherty, D.A. Stauffer, Acetylcholine binding by a synthetic receptor: implications for biological recognition, Science 250 (1990) 1558–1560.

[25] L.J. Andrews, R.M. Keefer, Molecular Complexes in Organic Chemistry, Holden-Day, San Francisco, 1964.

[26] G.C. Pimentel, A.L. McClellan, The Hydrogen Bond, W.H. Freeman, San Francisco, 1960.

[27] A.S. Reddy, H. Zipse, G.N. Sastry, Cation–π interactions of bare and coordinatively saturated metal ions: contrasting structural and energetic characteristics, J. Phys. Chem. B 111 (2007) 11546–11553.

[28] D. Vijay, G.N. Sastry, Exploring the size dependence of cyclic and acyclic π-systems on cation–π binding, Phys. Chem. Chem. Phys. 10 (4) (2008) 582–590.

[29] D. Vijay, H. Zipse, G.N. Sastry, On the cooperativity of cation–π and hydrogen bonding interactions, J. Phys. Chem. B 112 (30) (2008) 8863–8867.

[30] L.K. Engerer, T.P. Hanusa, Geometric effects in olefinic cation–π interactions with alkali metals: a computational study, J. Org. Chem. 76 (2011) 42–49.

[31] M. Levitt, M.F. Perutz, Aromatic rings act as hydrogen bond acceptors, J. Mol. Biol. 201 (1988) 751–754.

[32] J.Y. Lee, Molecular clusters of π-systems: theoretical studies of structures spectra and origin of interaction energies, Chem. Rev. 100 (2000) 4145–4185.

[33] J.B.O. Mitchell, C.L. Nandi, I.K. McDonald, J.M. Thornton, S.L. Price, Amino–aromatic interactions in proteins—is the evidence stacked against hydrogen bonding, J. Mol. Biol. 239 (1994) 315–331.

[34] H. Minoux, C. Chipot, Cation–π interactions in proteins: can simple models provide an accurate description? J. Am. Chem. Soc. 121 (1999) 10366–10372.

[35] M.J. Frisch, G.W. Trucks, H.B. Schlegel, G.E. Scuseria, M.A. Robb, J.R. Cheeseman, G. Scalmani, V. Barone, B. Mennucci, G.A. Petersson, H. Nakatsuji, M. Caricato, X. Li, H.P. Hratchian, A.F. Izmaylov, J. Bloino, G. Zheng, J.L. Sonnenberg, M. Hada, M. Ehara, K. Toyota, R. Fukuda, J. Hasegawa, M. Ishida, T. Nakajima, Y. Honda, O. Kitao, H. Nakai, T. Vreven, J.A. Montgomery, J.E. Peralta Jr., F. Ogliaro, M. Bearpark, J.J. Heyd, E. Brothers, K.N. Kudin, V.N. Staroverov, T. Keith, R. Kobayashi, J. Normand, K. Raghavachari, A. Rendell, J.C. Burant, S.S. Iyengar, J. Tomasi, M. Cossi, N. Rega, J.M. Millam, M. Klene, J.E. Knox, J.B. Cross, V. Bakken, C. Adamo, J. Jaramillo, R. Gomperts, R.E. Stratmann, O. Yazyev, A.J. Austin, R. Cammi, C. Pomelli, J.W. Ochterski, R.L. Martin, K. Morokuma, V.G. Zakrzewski, G.A. Voth, P. Salvador, J.J. Dannenberg, S. Dapprich, A.D. Daniels, O. Farkas, J.B. Foresman, J.V. Ortiz, J. Cioslowski, D.J. Fox, Gaussian 09, Revision B.01, Gaussian, Inc., Wallingford, CT, 2010.

[36] G.D. Purvis, R.J. Bartlett, A full coupled-cluster singles and doubles model: the inclusion of disconnected triples, J. Chem. Phys. 76 (1982) 1910–1919.

[37] T.J. Lee, J.E. Rice, An efficient closed-shell singles and doubles coupled-cluster method, Chem. Phys. Lett. 23 (1988) 406–415.

[38] G.E. Scuseria, H.F. Schaefer III, Is coupled cluster singles and doubles (CCSD) more computationally intensive than quadratic configuration interaction (QCISD)? J. Chem. Phys. 90 (1989) 3700–3703.

[39] G.E. Scuseria, C.L. Janssen, H.F. Schaefer III, An efficient reformulation of the closed-shell coupled cluster single and double excitation (CCSD) equations, J. Chem. Phys. 89 (1988) 7382–7388.

[40] S. Miertus, E. Scrocco, J. Tomasi, Electrostatic interaction of a solute with a continuum. A direct utilization of ab initio molecular potentials for the prevision of solvent effects, Chem. Phys. 55 (1981) 117–129.

[41] C. Amovilli, V. Barone, R. Cammi, E. Cances, M. Cossi, B. Mennucci, C.S. Pomelli, J. Tomasi, Recent advances in the description of solvent effects with the polarizable continuum model, Adv. Quant. Chem. 32 (1998) 227–262.

[42] M. Cossi, V. Barone, Analytical second derivatives of the free energy in solution by polarizable continuum models, J. Chem. Phys. 109 (1998) 6246–6254.

[43] J.B. Foresman, T.A. Keith, K.B. Wiberg, J. Snoonian, M.J. Frisch, Solvent effects. 5. Influence of cavity shape truncation of electrostatics, and electron correlation on ab initio reaction field calculations, J. Phys. Chem. 100 (1996) 16098–16104.

[44] T. Kar, J. Pattanayak, S. Scheiner, Insertion of lithium ions into carbon nanotubes: an ab initio and DFT study, J. Phys. Chem. A 105 (2001) 10397–10403.

[45] Q. Li, T. Hu, X.L. An, W.Z. Li, J.B. Cheng, B.A. Gong, J.Z. Sun, Theoretical study of the interplay between lithium bond and hydrogen bond in complexes involved with HLi and HCN, ChemPhysChem 10 (2009) 3310–3315.